*J. Phys. Chem. A* **1998,** *102,* 8037−8043

# UV-Photoelectron, Electron Transmission, and Dissociative Electron Attachment Spectroscopies of Acetone Oximes

**Maurizio Dal Colle and Giuseppe Distefano***

*Dipartimento di Chimica, Università di Ferrara, Via Borsari 46, 44100 Ferrara, Italy*

**Alberto Modelli**

*Dipartimento di Chimica "G. Ciamician", Universita di Bologna, 40127 Bologna, Italy*

**Derek Jones and Maurizio Guerra**

*ICoCEA, Consiglio Nazionale delle Ricerche, Bologna, Italy*

**Paulo R. Olivato and Douglas da Silva Ribeiro**

*Instituto de Química, Universidade de São Paulo, Brazil*

*Received: April 21, 1998; In Final Form: June 29, 1998*

The conformation and the electronic structure of several α-heterosubstituted acetone oximes $XCH_2(CH_3)C{=}NOH$ (X = H (**1**), F (**2**), Cl (**3**), $CH_3O$ (**4**), $C_2H_5S$ (**5**), and $(CH_3)_2N$ (**6**)) have been determined by means of a multidisciplinary approach based on ultraviolet photoelectron (UP), electron transmission (ET), and dissociative electron attachment (DEA) spectroscopies and fully optimized ab initio 6-31G** and MP2/6-31G** calculations. The vertical ionization energy (IE) and electron affinity (EA) values related to the HOMO ($\pi_{C=N}$) and LUMO ($\pi^*_{C=N}$) have been determined by the ΔSCF and ΔMP2 (IE only) procedures. The compounds studied prefer an anti (*E*) configuration between the OH and the $CH_2X$ group and a gauche conformation of the C−X bond with respect to the double bond, except **2** and **4** for which a syn (*Z*) planar structure is nearly degenerate with the *E* one. The spectral data, coupled with the results of the calculations, indicate that the properties of the acetone oximes are mainly governed by the mixing between the orbitals localized at the X and C=N fragments and by electrostatic interactions between hydrogen and the electronegative atoms. When X has poor donor and poor mesomeric acceptor properties (X = F and OMe), the prevailing interaction is the strong charge-transfer mixing of the hydroxyl oxygen lone pair with the $\pi^*_{C=N}$ orbital and the X group moves in the main molecular plane.

## Introduction

For several years we have studied the preferred conformation of organic carbonyl compounds by means of a multidisciplinary approach based on the experimental determination of filled and empty MO energies and, in some cases, of the molecular structure by X-ray diffraction analysis, coupled with theoretical calculations of geometrical parameters, orbital energies, and charge density distributions. The preferred conformation results not only from a balance of mesomeric, charge transfer (CT), electrostatic, and steric interactions between groups which are directly bonded, but also from the nature of remote substituents which modify the charge density on the bonding atoms of those groups. Thus, the nature of the minimum energy conformation is not always predictable a priori. For example, in ω-halogenoacetophenones, $p\text{-}YC_6H_4C(O)CH_2X$, we have found that the *para* substituent affects the interaction between the $CH_2{-}X$ and CO groups by modifying the electronic structure of the latter without varying its steric environment.[1] An additional example is the comparison of UP and ET spectra of α-phenylthioacetones, $p\text{-}XC_6H_4SCH_2C(O)CH_3$,[2] with those of α-phenylthioacetonitriles, $p\text{-}XC_6H_4SCH_2CN$.[3] Two groups of conformers are discernible in the UP spectra of both series of compounds. The conformers differ due to the varying degree of interaction between the sulfur lone pair and the ring π orbitals. However, in the acetonitriles, there is only one rotamer when X is an electron-releasing substituent, while in the acetyl derivatives this occurs only when the substituent has strong electron-withdrawing properties. This outcome results from a sort of competition between the two substituents interacting with the sulfur atom. The sum of the interactions produces a delicate geometric compromise which can be unbalanced by variation of a remote substituent.[2] More recently, we have observed that in β-thiocarbonyl derivatives ($YC(O)CH_2S(O)_nR$, $n = 0{-}2$), the orientation of the $CH_2{-}S$ bond with respect to the main plane of the carbonyl group depends on the interaction between the group orbitals of the two fragments (Y(CO) and $S(O)_nR$) as a function of Y and R ($n = 0$),[4] as well as on the electrostatic interactions between pairs of oppositely charged atoms $O/S(O)_n{-}O/C(O)$ and/or $C/C(O){-}S$ ($n = 1$[5] and 2[6]) and on the steric hindrance of R ($n = 1$[7]).

In the present paper, we present the results of a combined experimental (UPS, ETS and DEAS) and theoretical (HF/6-31G** and MP2/6-31G**) approach to the study of the preferred conformation of some α-heterosubstituted acetone oximes listed in Scheme 1. The aim of the present work is to determine the influence of the remote OH substituent on the preferred

S1089-5639(98)01924-0 CCC: $15.00

**SCHEME 1**

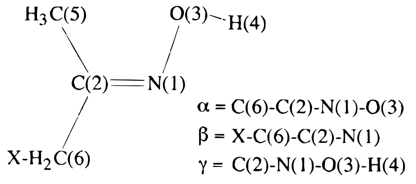

X = **1** H, **2** F, **3** Cl, **4** $CH_3O$, **5** $C_2H_5S$, **6** $(CH_3)_2N$

orientation of the $CH_2{-}X$ bond and to compare the gas-phase conformations with the results of recent condensed-phase analyses,[8] which have indicated that the above compounds adopt the *E* configuration, that all except the fluorine derivative have a gauche conformation, and that there is no intramolecular X- - - H/OH hydrogen bonding.

## Experimental Section

**UP Spectra.** The He(I) photoelectron spectra were recorded on a Perkin-Elmer PS-18 photoelectron spectrometer connected to a Datalab DL4000 signal analysis system. The bands, calibrated against rare-gas lines, were located using the position of their maxima, which were taken as corresponding to the vertical IE values. The accuracy of the IE values was estimated to be better than 0.05 eV (except for shoulders). The assignment of the spectra is based on the composite-molecule approach and the substituent effect, using the unsubstituted acetoneoxime **1**[9] and the methyl derivatives of the X substituents $CH_3F$, $CH_3Cl$, $(CH_3)_3N$, $CH_3OCH_3$,[10] and $CH_3SC_2H_5$[11] as reference compounds. The samples were available from previous studies.[8]

**ET and DEA Spectra.** Electron transmission spectroscopy takes advantage of the sharp variations in the total electron−molecule scattering cross-section caused by resonance processes, that is, the formation of temporary anion states. The energies (AEs) at which electron attachment occurs correspond to the negative of the vertical electron affinities (EAs). Our electron transmission apparatus is in the format devised by Sanche and Schulz[12] and has been previously described.[13] To enhance the visibility of the sharp resonance structures, the impact energy of the electron beam is modulated with a small ac voltage and the derivative (with respect to the electron impact energy) of the electron current transmitted through the gas sample is measured directly by a synchronous lock-in amplifier. The present spectra have been obtained by using the apparatus in the "high-rejection" mode[14] and are, therefore, related to the nearly total scattering cross-section. The electron beam resolution was about 50 meV (fwhm). The energy scales were calibrated with reference to the $(1s^12s^2)^2S$ anion state of He. The estimated accuracy is ± 0.05 or ± 0.1 eV, depending on the number of decimal digits reported.

In our apparatus the collision chamber has been modified in order to allow for ion extraction at 90° with respect to the electron beam direction. The collision chamber is divided into two-half-cylinders which can generate an extraction field of about 0.45 V/cm. Ions are then accelerated and focused toward the entrance of a quadrupole mass filter. A more detailed description is reported in ref 15. Alternatively, the two halves of the collision chamber can be electrically shorted, with no voltage applied, to collect the total anion current, which is measured with a Keithley 485 picoammeter. The present DEA data were obtained with an electron beam current about 4 times as large as that used for the ET experiment. The energy spread of the electron beam, as evaluated from the $SF_6^-$ signal in $SF_6$ (used for calibration of the energy scales), increased to about 100 meV. For all samples, the DEA data have been recorded with the same pressure reading ($2 \times 10^{-5}$ mbar, measured in the main vacuum chamber by means of a cold cathode ionization gauge). Preliminary measurements showed that the total anion current reading is proportional to the pressure, at least in the $10^{-5}{-}(4 \times 10^{-5})$ mbar range.

**Calculations.** The valence orbital energy and localization properties, the electron charge distribution at the various atoms, and the geometric parameters for compounds **1**−**6** and for formaldoxime ($H_2C{=}NOH$) were computed at the HF/6-31G** level using the Gaussian 94[16] series of programs. To determine the preferred conformation, we fully optimized at the HF/6-31G** level several starting geometries in which the OH group is syn ($Z$, $\alpha = C(6){-}C(2){-}N(1){-}O(3) = 0°$) or anti ($E$, $\alpha = 180°$) with respect to the substituted methyl group, the C−X bond lies in the molecular plane cis ($c$, $\beta = X{-}C(6){-}C(2){-}N(1) = 0°$) or trans ($t$, $\beta = 180°$) to the double bond or outside the molecular plane (gauche, *g*), and the hydrogen atom of the OH group is cis ($c$, $\gamma = C(2){-}N(1){-}O(3){-}H(4) = 0°$ or trans ($t$) to the double bond. Only two gauche minima have been obtained for the chlorine derivative. These minima, the minimum found for the unsubstituted compound, and the four most stable ones for the remaining substituted acetone oximes have been optimized at the MP2 level. The energy minima are labeled with the symbols appropriate to the values of the α, β, and γ angles, in that order: e.g., **2***E*(*g*,*t*) indicates that in the considered minimum of the fluorine derivative (**2**), the OH group is anti to the $CH_2F$ group (α), the C−F bond is outside the main molecular plane (β), and the H/OH atom is trans to the double bond (γ). The vertical ionization-energy values related to the HOMO of **1**−**6** were computed with the ΔSCF and ΔMP2 procedures at the MP2/631-G** optimized geometries, while the vertical AE values of the LUMO ($\pi^*_{C=N}$) were obtained at the ΔSCF level. In fact, preliminary calculations of the AE for the unsubstituted compound at the MP2 level indicated that the electron correlation energy effect is rather small (0.16 eV), so that the AE values at this level have not been computed. To save computer time, the ethyl group of **5** has been substituted with a methyl group.

## Results and Discussion

**Geometry.** The relevant geometrical parameters computed at the MP2/6-31G** level for acetone oxime (**1**), formaldoxime ($H_2C{=}NOH$), and for the most stable conformer (*E*(*g*,*t*)) of dimethylamino acetone oxime (**6**) are collected in Table 1 together with the corresponding experimental data.[17−19] Acetone oxime prefers a $C_s$, symmetry, where H(9) and H(4) adopt a trans conformation, while H(11) prefers a cis one with respect to the C=N double bond (see Scheme 2). The X-ray structure of **1** was obtained[17] for a planar trimer having fairly strong intermolecular OH- - -N, bonds and the geometric data deviate[17] from accepted average crystallographic values.[18] On the other hand, the computed data agree with the computed and experimental values for formaldoxime and dimethylaminoacetone oxime (see Table 1). The latter compound, in particular, prefers an anti configuration where the $Me_2N{-}C$ bond is outside the main molecular plane (gauche conformation). The molecular residue is planar, the torsion angle C(5)−C(2)−N(1)−O(3) (−0.08°) having a value close to the X-ray one (−0.04°).[8] The angles around the amino nitrogen are about 110°, indicating an evident pyramidization, in agreement with experimental data. The present calculations, therefore, accurately reproduce the geometry of this class of compounds and can be used to analyze differences caused by the substituents.

**TABLE 1: Theoretical (MP2/6-31G**) and Experimental Bond Distances (Å) and Angles (deg) for Oximes**

| | acetoneoxime | | | formaldoxime | | $Me_2N$−acetoxime[$E(g,t)$] | |
|---|---|---|---|---|---|---|---|
| | Th | X-ray[a] | X-ray[b] | Th | MW[c] | Th | X-ray[d] |
| N(1)═C(2)[e] | 1.291 | 1.29 | 1.280 | 1.284 | 1.276 | 1.291 | 1.278 |
| N(1)−O(3) | 1.420 | 1.36 | 1.418 | 1.409 | 1.408 | 1.417 | 1.400 |
| O(3)−H(4) | 0.966 | | | 0.966 | 0.956 | 0.966 | |
| C(2)−C(5) (H(5)) | 1.500 | 1.49 | | 1.084 | 1.085 | 1.497 | 1.484 |
| C(2)−C(6)(H(6)) | 1.498 | 1.55 | 1.50−1.51 | 1.079 | 1.086 | 1.501 | 1.500 |
| N(12)−C(6) | | | | | | 1.461 | 1.469 |
| N(12)−C(13) | | | | | | 1.456 | 1.470 |
| N(12)−C(14) | | | | | | 1.458 | 1.465 |
| N(1)−O(3)−H(4) | 101.10 | 111 | | 101.81 | 102.7 | 101.202 | |
| C(2)−N(1)−O(3) | 110.04 | 111 | | 109.92 | 110.2 | 110.288 | 112.5 |
| N(1)−C(2)−C(5) | 123.41 | 131 | | 122.69 | 121.8 | 124.615 | 125.2 |
| N(1)−C(2)−C(6) | 116.15 | 113 | | 116.28 | 115.6 | 115.547 | 115.6 |
| C(2)−C(6)−N(12) | | | | | | 110.852 | 113.6 |
| C(6)−N(12)−C(13) | | | | | | 110.415 | 108.8 |
| C(6)−N(12)−C(14) | | | | | | 110.594 | 111.4 |
| C(13)−N(12)−(14) | | | | | | 110.225 | 109.6 |

[a] From ref 18. [b] Average crystallographic data for oximes from ref 19. [c] Microwave data from ref 19. [d] From ref 8. [e] See Scheme 1 for atom numbering.

**SCHEME 2**

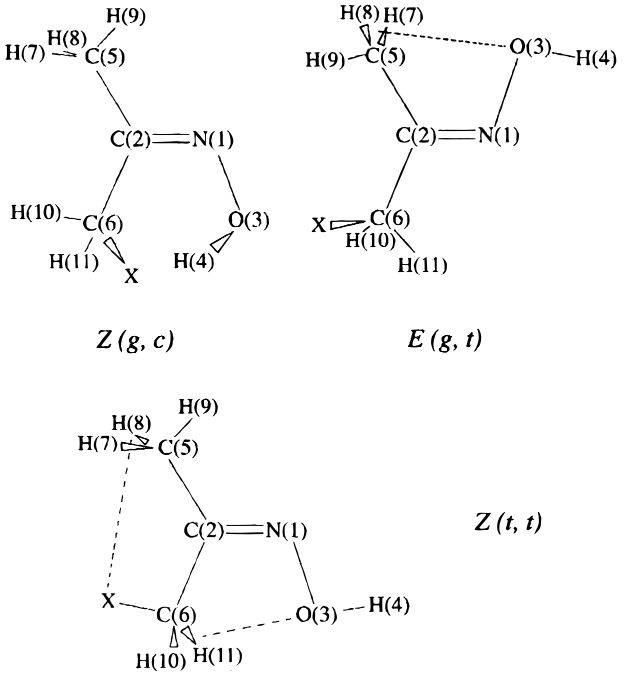

The value for the dihedral angles α, $\beta$, and $\gamma$ for compounds **2**−**6** are listed in Table 2. The minima are labeled with the symbols defined above, and their relative energy is quoted. In general, the most stable minimum is $E(g,t)$ (see Scheme 2) except for **2**, which prefers a trans conformation ($Z(t,t)$, see below). The $E(g,t)$ minimum is stabilized by crossed charge transfer (CT) interactions between the orbitals localized at the C−X and the double bonds, which favor the gauche conformation. It is further stabilized by an electrostatic interaction between the negatively charged oxygen atom ($q_O \approx -0.53$ e) and one or two hydrogen atoms ($q_H = +0.17$ e) of the syn $CH_3$ group which are away from O(3) ($d_{H-O} = 2.5-2.6$ Å), less than the sum of the corresponding van der Waals radii (2.72 Å).[19]

The Z($t,t$) minimum has the same energy as $E(g,t)$ in **4** and is slightly (1.33 kJ/mol) more stable in **2**. The change of the relative energy of the two minima with respect to compounds **3**, **5**, and **6** derives from the activation in the $Z(t,t)$ structure (see Scheme 2) of the electrostatic interactions O(3)- - -H(10, 11) ($d_{O(3-H(10,11)} \approx 2.53$ Å, $q_O \approx -0.55$ e, $q_H \approx 0.15$ e) and X- - -H(7,8) ($d_{X-H(7,8)} \approx 2.67$ Å, $q_O \approx -0.65$ e, $q_F \approx -0.42$ e, $q_H \approx 0.14$ e) and from a reduction of the $\sigma_{C-X}/\pi_{CN}$ mixing when the substituent contains a highly electronegative second-row element such as fluorine and oxygen. In fact, the C−OMe and C−F filled MO's lie deeper[10] and the corresponding virtual orbitals are much higher[20−24] in energy than those of the corresponding third-row derivatives.

**TABLE 2: Relative Energy (kJ mol$^{-1}$) and Selected Dihedral Angles (deg) for Different Structures of Substituted Acetoneoximes $XCH_2(CH_3)C{=}NOH$ at the MP2/6-31G** Level**

| X | structures | $\Delta E$ | α[a] | $\beta$ | $\gamma$ |
|---|---|---|---|---|---|
| **2** (F) | $E(g,t)$[b] | 1.33 | 176.7 | 128.7 | 177.5 |
| | $Z(t,t)$ | 0.00 | 0.0 | 180.0 | 180.0 |
| | $E(c,t)$ | 12.39 | 180.0 | 0.0 | 180.0 |
| | $Z(g,c)$ | 27.43 | 3.1 | −52.3 | 23.5 |
| **3** (Cl) | $E(g,t)$ | 0.00 | 178.7 | 116.8 | 179.4 |
| | $Z(g,t)$ | 5.14 | 0.4 | 99.3 | −179.6 |
| **4** (MeO) | $E(g,t)$ | 0.00 | 177.8 | 125.5 | 178.2 |
| | $Z(t,t)$ | 0.00 | 0.0 | 179.9 | 180.0 |
| | $E(c,t)$ | 15.25 | 180.1 | −0.4 | 180.0 |
| | $Z(g,c)$ | 17.10 | 3.0 | −55.9 | 26.6 |
| **5** (SMe)[c] | $E(g,t)$ | 0.00 | 179.8 | 111.8 | 179.6 |
| | $Z(g,t)$[d] | 1.94 | −0.5 | −92.5 | 179.4 |
| | $Z(g,t)$[d] | 2.99 | 0.0 | 78.6 | −179.3 |
| | $E(c,t)$ | 5.95 | 180.0 | 0.0 | 180.0 |
| **6** ($Me_2N$) | $E(g,t)$ | 0.00 | 178.4 | 122.3 | 179.0 |
| | $Z(g,t)$ | 5.63 | 0.4 | 109.9 | 179.6 |

[a] The angles α, $\beta$, and $\gamma$ are defined in Scheme 1. [b] The labels for the minima have been defined in the Experimental Section. [c] Me represents a $CH_3$ group; to save computer time, the calculations were carried out on the $SCH_3$ derivative instead of the $SC_2H_5$ one. [d] The two $Z(g,t)$ structures of **5** differ for the orientation of the Me/SMe group (C(1)−C(6)−S−Me = 187.0°, lower energy configuration, or 68.7°).

An additional structure peculiar to second-row substituents is $Z(g,c)$ (see Scheme 2). It is the only minimum in which the H(4) atom ($q_H \approx 0.14$ e) is cis to the double bond because of a strong electrostatic interaction with X ($q_X \approx -0.42$ (F) and −0.65 (O) e; $d_{X-H(4)} \approx 1.85$ Å). The severe X/H(4) steric hindrance, however, pushes the two atoms out of the main molecular plane in opposite directions (−54° (X) and +25° (H(4)). The value of the X- - -H−O angle (145−146°), the increase of the O−H distance (0.973 (**2**) and 0.978 (**4**) Å) with respect to the $E(g,t)$ structures ($d_{O-H} = 0.966$ Å (**2** and **4**)), and the short X- - -OH distance (ca. 2.71 Å) indicate[25,26] the presence

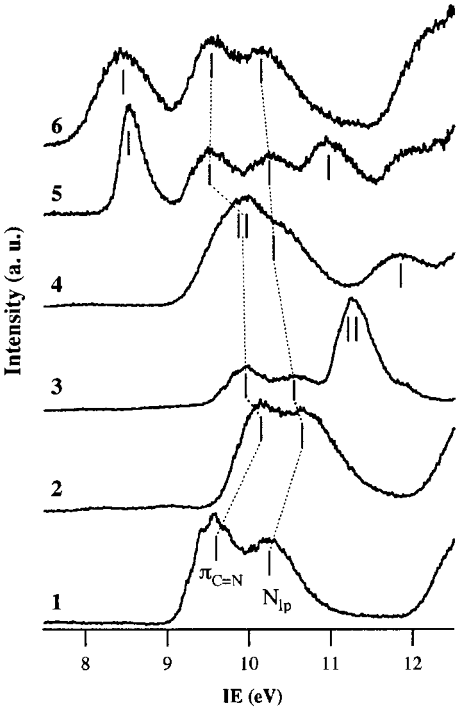

**Figure 1.** Photoelectron spectra of substituted acetone oximes $XCH_2$-$(CH_3)C{=}NOH$ (X = H (**1**), F (**2**), Cl (**3**), $CH_3O$ (**4**), $C_2H_5S$ (**5**), and $(CH_3)_2N$ (**6**)).

of intramolecular hydrogen bonding. However, owing to the high energy (and low population) of the *Z*(*g*,*c*) structures with respect to the *E*(*g*,*t*) ones (see Table 2), no experimental evidence is expected for this intramolecular interaction, in agreement with IR data in diluted solutions.[8] The rotation of the OH group out of the main molecular plane, however, decreases the stabilizing $\pi^*_{CN} \leftarrow$ oxygen lone pair ($O_{lp}$) CT interaction contributing, together with the X/H(4) steric hindrance, to the large energy increase with respect to the absolute minimum (see Table 2).

Finally, the low-energy minimum common to all the derivatives (except **3**) is *E*(*c*,*t*) in which the heterosubstituent lies in the main molecular plane cis to the double bond. The *E*(*c*,*t*) minimum has a relatively high energy with respect to the most stable structure, except in **5** ($\Delta E = 5.95$ kJ/mol) because of a CT interaction between the HOMO of the planar $C_2H_5S$ fragment ($S_{lp}$) and the $\pi^*_{C=N}$ orbital. The *Z*(*g*,*c*) and the *E*(*c*,*t*) minima have been also observed for the $N(CH_3)_2$ derivative at the HF/6-31G** level.

**UP Spectra.** The low IE region of the UP spectra of derivatives **1**−**6** is presented in Figure 1. The IE values lower than about 12 eV are collected in Table 3 together with the corresponding HF/6-31G** MO energies (KT), the first IE values computed with the ΔSCF and ΔMP2 methods, and the relevant data from the spectra of the reference compounds **2a**−**6a**. The two bands present in the low IE region of the spectrum of **1** were ascribed[9] to the $\pi_{C=N}$ (9.60 eV) and the nitrogen lone pair ($N_{lp}$, 10.25 eV) MO's[27], the former with a partially resolved vibrational structure being slightly more intense. Eigenvector analysis indicates that both MO's are mixed with the appropriate $O_{lp}$ orbital of the OH group.

The corresponding bands in the spectra of **2**−**6**, occurring between 9.5 and 10.65 eV, show the stabilizing inductive effect exerted by the substituent when X = Cl, $CH_3O$, and F (see Figure 1). Eigenvector analysis shows contributions from the X-group orbitals which are larger for substituents containing third-row elements and smaller for the more electronegative groups, in agreement with the above-mentioned decrease of the $\pi_{C=N}/\sigma_{C-X}$ hyperconjugative interactions for the latter.

**TABLE 3: Valence Region Experimental IE Values (eV) for Compounds 1−6 and Reference Molecules 2a−6a, and Corresponding Data Computed for Compounds 1−6 at Different Levels Using the 6-31G** Basis Set: HF-Koopmans (KT), HF-ΔSCF, and ΔMP2**

| | | | $X_{lp1}$ | $\pi_{C=N}$ | $N_{lp}$ | $X_{lp2}$ |
|---|---|---|---|---|---|---|
| **1** | $CH_3(CH_3)C{=}NOH$ | exp | | *9.60* | *10.25* | |
| | | KT | | 10.01 | 11.62 | |
| | | ΔSCF | | 8.47 | | |
| | | ΔMP2 | | 9.42 | | |
| **2** | $FCH_2(CH_3)C{=}NOH$ | exp | *a* | *10.15* | *10.65* | |
| | *Z*(*t*,*t*) | KT | | 10.46 | 11.98 | |
| | | ΔSCF | | 8.94 | | |
| | | ΔMP2 | | 9.83 | | |
| | *E*(*g*,*t*) | KT | | 10.55 | 12.10 | |
| | | ΔSCF | | 9.03 | | |
| | | ΔMP2 | | 9.93 | | |
| **2a** | $CH_3F$[b] | exp | *13.04* | | | *13.04* |
| **3** | $ClCH_2(CH_3)C{=}NOH$ | exp | *11.26* | *9.96* | *10.55* | *11.26* |
| | *E*(*g*,*t*) | KT | 12.02 | 10.50 | 11.92 | 12.38 |
| | | ΔSCF | | 8.93 | | |
| | | ΔMP2 | | 9.76 | | |
| **3a** | $CH_3Cl$[b] | exp | *11.29* | | | *11.29* |
| **4** | $MeOCH_2(CH_3)C{=}NOH$ | exp | *9.92* | *9.92* | *10.3* | *11.85* |
| | *E*(*g*,*t*) | KT | 11.82 | 10.19 | 11.66 | 13.38 |
| | | ΔSCF | | 8.59 | | |
| | | ΔMP2 | | 9.51 | | |
| | *Z*(*t*,*t*) | KT | 11.87 | 10.07 | 11.62 | 13.47 |
| | | ΔSCF | | 8.49 | | |
| | | ΔMP2 | | 9.49 | | |
| **4a** | $(Me)_2O$[b] | exp | *10.04* | | | *11.91* |
| **5** | $EtSCH_2(CH_3)C{=}NOH$ | exp | *8.53* | *9.52* | *10.25* | *10.97* |
| | *E*(*g*,*t*) | KT | 9.30 | 10.10 | 11.82 | 12.12 |
| | | ΔSCF | 7.69 | | | |
| | | ΔMP2 | 8.39 | | | |
| **5a** | EtSMe[c] | exp | *~8.5* | | | *~11.0* |
| **6** | $Me_2NCH_2(CH_3)C{=}NOH$ | exp | *8.46* | *9.54* | *10.15* | |
| | *E*(*g*,*t*) | KT | 9.89 | 10.10 | 11.63 | |
| | | ΔSCF | 7.53 | | | |
| | | ΔMP2 | 8.42 | | | |
| **6a** | $Me_3N$[b] | exp | *8.44* | | | |

[a] The $F_{lp}$ bands have not been identified in the spectra. [b] From ref 10. [c] Average data from $(CH_3)_2S$ (8.67 and 11.2 eV) and $(C_2H_5)_2S$ (8.44 and 10.7 eV, ref 11).

The spectra also exhibit the band(s) related to ionization from the X heteroatom lone pair(s) at nearly the same energy as in the spectra of the corresponding reference compounds (see Table 3), indicating that the inductive stabilization caused by the oxime fragment is nearly balanced by orbital mixing.

The use of Koopmans' Theorem ($IE_i = -\epsilon_i$)[28] to reproduce the energetics of the molecular ionization processes involves two approximations: namely, the neglect of electron relaxation energy and the change in electron correlation energy associated with the removal or the addition of an electron. In the following, we present a simple estimation of the change in each of the above-cited energies independently from each other, along the series **1**−**6**. We assume that the chemical systems under consideration can be described by a single Slater determinant wave function, even in the ionic states. Because of the crude approximation and of the small basis set used in our approach, we do not attach any quantitative meaning to the data reported below. Their trends, however, are in line with the present experimental evidence and with other spectroscopic properties[8] of the studied compounds.

The ΔSCF procedure between the neutral optimized ground state and the positively ionized state at the neutral molecule geometry provides the value for the vertical ionization energy in which electron relaxation is taken into account. The computed ($IE_{th}$) values, therefore, when compared with the experimental ones (IE), provide information on the difference between the electron correlation energy ($\Delta E_{corr}$) of the neutral and cation states. In fact, IE > $IE_{th}$ (see Table 3), indicating that the neutral system has a larger correlation energy than the positive ion, as generally assumed, and that the neglect of electron correlation energy is the dominant error in the computed values. As reported above, the HOMO of compounds **1**−**4** is mainly localized at the double bond with a sizable contribution from the $O_{lp}$ orbital and a variable one from the C−X group, the latter contribution being the largest for **3**. In **3**, therefore, the region of space shared by the electrons in the double bond and those on the X substituent is larger than in the other three derivatives (the F atom, in fact, lies in the main molecular plane and the H and O atoms are smaller than chlorine). In other words, the $\Delta E_{corr}$ between the electrons of the double bond and those of X is the largest in **3**. This naive picture requires a larger reduction of $\Delta E_{corr}$ upon $\pi$-ionization for **3** than for the other derivatives. This expectation is in agreement with the observed trend of the IE − $IE_{th}$ differences, namely, Cl (1.03) < H (1.13) < F (1.21) < O (1.33 eV) (see Table 3).

The first IE value for **1**−**6** is closely reproduced by estimating the correlation energy at the simple MP2 level (see Table 3), the deviation being smaller than 0.4 eV. We have previously observed[5,29] that ground-state ab-initio calculations reproduce IE values more closely for $\pi$ MO's than for lone pair MO's, the latter being computed, in the Koopmans' theorem approximation, to be too stable by 1−2 eV. This different behavior has been tentatively ascribed to the larger electron relaxation accompanying ionization from a localized AO than from a delocalized $\pi$ MO. Electron relaxation is taken into account by ΔSCF calculations, whereas ΔMP2 calculations take into account both electron relaxation and the correlation energy so that to a first approximation a comparison between the KT, ΔSCF, and ΔMP2 IE values could shed some light on the validity of the KT approximation. The data of Table 3 indicate that the variation of electron correlation, as measured from (ΔMP2 − ΔSCF), increases the IE values by about 1 eV while the electron relaxation (KT − ΔSCF) decreases the IE values by a similar amount (1.5 eV) for the $\pi$-ionization, so that the Koopmans' approximation provides good IE values. On the other hand, as expected, the electron relaxation is larger for lone pair ionization, so that the KT values are in poor agreement with experiment. The electron relaxation for lone pair orbitals does, in fact, increase with the heteroatom hardness. Indeed, the difference between KT and experimental $X_{lp}$ IE values increases in the order S, Cl (ca. 0.8) ≪ N (1.43) < O (1.9 eV).

**ET and DEA Spectra.** The electron transmission spectra of acetone oximes **1**−**6** are shown in Figure 2, and the measured vertical electron attachment energy (AE) values are reported in Table 4. The sharp resonance at 2.01 eV in the spectrum of **1** is ascribed to electron capture into the $\pi^*_{C=N}$ MO, considering that the corresponding $\pi^*_{C=N}$ AE occurs at 1.29 eV in di-*tert*-butylimine ($t\text{-}Bu_2C{=}NH$)[30], that replacement of the *tert*-butyl groups with methyl groups desatabilizes the $\pi^*_{C=O}$ MO by 0.32 eV,[30,31] and that the OH group destabilizes adjacent $\pi^*$ orbitals by ca. 0.5 eV.[24] In Figure 3 the HF/6-31G** (KT) energies and the vertical AE values ($AE_v$) computed by ΔSCF calculations for the $\pi^*_{C=N}$ levels are reported together with the experimental AE values. For compounds **2** (X = F) and **4** (*X* = MeO), the computed LUMO energies for the two nearly isoenergetic structures *Z*(*t,t*) and *E*(*g,t*) are shown. A comparison with the experimental trend suggests that the preferred conformations are *Z*(*t,t*) and *E*(*g,t*) for the fluorine and oxygen derivative, respectively. The peculiar trans orientation of the substituent in compound **2** (X = F) agrees with total energy calculations and solution data.[8] (In solution, however, the *E* configuration predominates also for **2**.) The stability of the $\pi^*_{C=N}$ MO increases with the (second-row) substituent electronegativity in the series **1** < **6** < **4** < **2**. The further increase observed when the X substituent contains a third-row element is ascribed to a larger $\pi^*_{C=N}/\sigma^*_{C-X}$ mixing, in agreement with previous observations on carbonyl,[1,23] aromatic,[3,13,22,24] and heteroaromatic[32] derivatives. The large stabilization observed going down the groups, despite the electronegativity decrease, indicates that

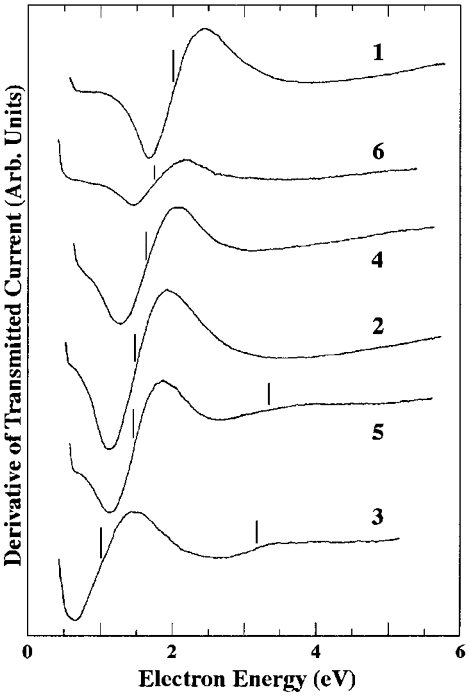

**Figure 2.** Derivative of the transmitted electron current for the gas-phase acetone oximes $XCH_2(CH_3)C{=}NOH$ (X = H (**1**), F (**2**), Cl (**3**), $CH_3O$ (**4**), $C_2H_5S$ (**5**), and $(CH_3)_2N$ (**6**)).

**TABLE 4: Resonance and Peak Energies (eV) Measured in the ET and DEA Spectra, Respectively, of the α-Heterosubstituted Acetone Oximes $XCH_2(CH_3)C{=}NOH$ (X = H (1), F (2), Cl (3), $CH_3O$ (4), $C_2H_5S$ (5), and $(CH_3)_2N$ (6)[a]**

| | | DEA | | | | |
|---|---|---|---|---|---|---|
| | ET | fragment anion current | | | total anion current | |
| compound | AE | fragment | peak energy | rel int | peak energy | rel int |
| 1 | 2.01 | | | | | |
| 2 | 1.48 | $F^-$ | 1.38 | 100 | 1.26 | 12 |
| | | $(M-F)^-$ | 1.02 | 60 | | |
| | | $M^-$ | 1.28 | 22 | | |
| | | $CH_2CN^-$ | 1.38 | 8 | | |
| 3 | 1.02 | $Cl^-$ | 0.82 | | 0.88 | 100 |
| | 3.2 | | | | | |
| 4 | 1.63 | $(M\text{-}OCH_3)^-$ | 1.44 | 100 | 1.50 | 2 |
| | | $OCH_3^-$ | 1.72 | 37.5 | | |
| | | $CH_2CN^-$ | 1.68 | 25 | | |
| | | $M^-$ | 1.74 | 12.5 | | |
| 5 | 1.46 | $SC_2H_5^-$ | 1.30 | 100 | 1.18 | 20 |
| | 3.4 | $(M\text{-}SC_2H_5)^-$ | 1.07 | 66.5 | | |
| | | $M^-$ | 1.33 | 2 | | |
| 6 | 1.78 | | | | | |

[a] The relative intensity values reported for the fragment anion currents represent the relative heights of the signals observed within each single compound, whereas the relative intensities reported for the total anion currents represent the ratios among the signals measured in the various compounds with the same vapor pressure. M represents the neutral molecule.

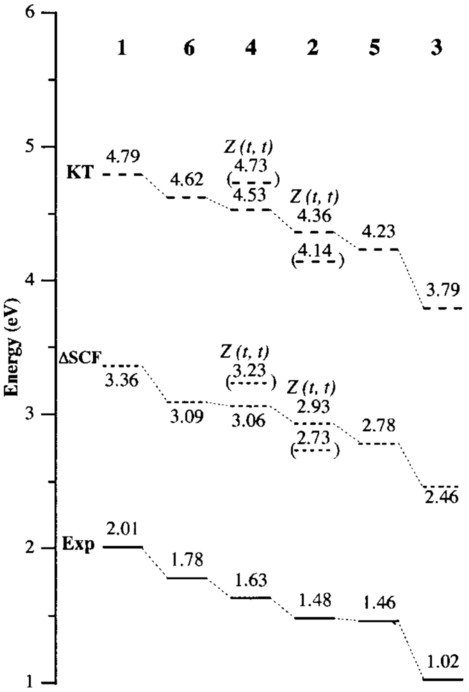

**Figure 3.** Correlation between experimental (—) and computed (KT (- - -) and ΔSCF (···)) $\pi^*$ AE values for acetone oximes $XCH_2(CH_3)C{=}NOH$ (X = H (**1**), F (**2**), Cl (**3**), $CH_3O$ (**4**), $C_2H_5S$ (**5**), and $(CH_3)_2N$ (**6**)). The computed values refer to the *E*(*g*,*t*) structure unless otherwise indicated.

the C−X bonds (X = Cl and $SCH_3$) are significantly outside the main molecular plane, in agreement with the conformational results reported above. The difference KT − ΔSCF is nearly constant (1.45 ± 0.1 eV), indicating that the electron relaxation energy does not depend on X. The LUMO, in fact, derives from the mixing of the empty $\pi^*_{C=N}$ and $\sigma^*_{C-X}$ orbitals with a fairly constant charge-transfer contribution from the $O_{lp}$ orbital.

Preliminary calculations of the vertical $\pi^*$ AE for the unsubstituted compound at the ΔMP2 level indicate that the electron correlation energy effect is rather small (0.16 eV), so that AE values at this level have not been computed. Therefore, the sizable difference between the theoretical and the experimental values ($AE_{(\Delta SCF)} - AE_{(exp)} \approx 1.4$ eV) is likely due to the lack of basis-set flexibility, which is difficult to improve given that the inclusion of diffuse functions in the attempt to better describe the extra electron does not lead to reliable results.[33] LCAO methods are, thus, unable to reproduce the absolute values of negative electron affinities and allow only comparison between experimental and theoretical trends.[33]

The temporary anions formed by resonant electron attachment normally decay via ejection of the extra electron, but they can also dissociate when suitable energetic conditions exist. In this case, the two processes compete with each other, the former decay channel being kinetically favored for higher lying anion states because of their shorter lifetime. Figure 4 shows the negative ions formed by dissociative electron attachment in the 0−4 eV energy range. The peak energies and the relative intensities are collected in Table 4. The dimethylamino and the unsubstituted compounds, which have the higher lying anion states, do not give rise to negative ions. The total anion current associated with the $\pi^*$ resonance increases by an order of magnitude on going from the fluorine to the chlorine derivative and on going from the oxygen to the sulfur derivative (see Table 4). The anion peak energies parallel those of the resonances observed in the ET spectra, being shifted about 0.2 eV lower in energy for the reason mentioned above. Most of these anions derive from rupture of the C−X bond, the $(M-X)^-$ anion appearing about 0.3 eV lower in energy than the corresponding $X^-$ anion. The relative abundance of $X^-$ increases with the atomic number of the heteroatom of the substituent, $Cl^-$ being the only ion observed in the chloroderivative, while a variety of negative fragments are present in the spectra of the fluorine, oxygen, and sulfur derivatives. Formation of the $X^-$ fragment is the result of intramolecular transfer of the electron captured by the double bond to the X moiety. Table 4 shows that $X^-$ production increases by more than 1 order of magnitude on going from **2** to **3** and from **4** to **5**. This electron transfer implies $\pi^*_{C=N}/\sigma^*_{C-X}$ mixing. The DEA spectra, thus, confirm the theoretical results which predict the gauche conformation as the most stable one for the third-row (S, Cl) derivatives with large heteroatom participation in the $\pi^*$ LUMO. As a final comment, it can be noticed that detection of the molecular anion (which implies a survival time of the order of 1 $\mu$s) at an energy higher than 1 eV is rather unusual. To ascertain if the molecular anion can be stabilized by three-body collisions in our experimental conditions, we measured the signals at $m/e = 19$ ($F^-$) and 91 ($M^-$) in the fluoroderivative by increasing the sample pressure up to 4 times. The ratio between the two signals, however, did not change. The relative abundance of $M^-$ with respect to the total ion current seems to indicate that the lifetime of the molecular anion increases for derivatives with small $\pi^*/\sigma^*$ mixing.

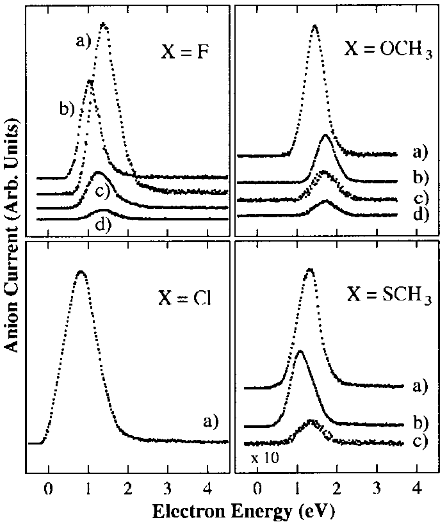

**Figure 4.** Dissociative electron-attachment spectra for acetone oximes $XCH_2(CH_3)C{=}NOH$ (X = F (**2**), Cl (**3**), $CH_3O$ (**4**), and $C_2H_5S$ (**5**)): (a) $X^-$, (b) $M{-}X)^-$, (c) $M^-$, (d) $CH_2CN^-$, where M represents the neutral molecule).

## Conclusions

The most stable conformations of α-heterosubstituted acetone oximes **1**−**6** have been determined by MP2/6-31G** calculations. For **1**, **3**, **5**, and **6** *E*(*g*,*t*) is the most stable structure, while for **2** and **4**, it is nearly degenerate with *Z*(*t*,*t*). The high electronegativity of the F and MeO substituents is responsible for both the occurrence of the *Z*(*t*,*t*) minimum, which is stabilized by strong electrostatic interactions, and the relative destabilization of the *E*(*g*,*t*) minimum due to the reduction of the X/$\pi$ hyperconjugative and charge-transfer interactions.

The variation of the $\sigma/\pi$-orbital mixing along the series is the main factor determining the main spectral features of this class of compounds. When the experimental $\pi_{C=N}$ IE values are compared with those obtained by the ΔSCF procedure, a trend for the variation of the electron correlation energy upon ionization is obtained (Cl < H < F < O), which is in agreement with the variation of the X/$\pi$ orbital mixing along the series. A comparison between the KT, $\Delta$SCF, and $\Delta$MP2 IE values indicates that the relaxation energy accompanying $X_{lp}$ ionization increases with the heteroatom hardness: S $\approx$ Cl $\ll$ N < O. On the other hand, the AE values clearly show the importance of the $\pi^*_{C=N}/\sigma^*_{C-X}$ mixing for third-row derivatives. While a comparison of the experimental AE trend with the results of the calculations indicates that *Z*(*t*,*t*) and *E*(*g*,*t*) are the most probable candidates for the lowest energy structures of **2** and **1** and **3**−**6**, respectively, in agreement with the results of the calculations. The relative abundance of the $X^-$ fragment deriving from electron capture in the $\pi^*_{C=N}$ LUMO increases in the order H, $(CH_3)_2N$ < $CH_3O$ < F < $C_2H_5S$ < Cl, that is by increasing the mixing between the X and the C=N group orbitals.

**Acknowledgment.** The authors acknowledge financial support from the MURST and the CNR. M.G. also acknowledges a contribution from the CNR "Progetto Strategico Modellistica Computazionale di Sistemi Molecolari Complessi".

## References and Notes

(1) Distefano, G.; Granozzi, G.; Bertoncello, R.; Olivato, P. R.; Guerrero, S. A. *J. Chem. Soc., Perkin Trans. 2* **1987**, 1459.

(2) Distefano, G.; Guerra, M.; Jones, D.; Modelli, A.; Olivato, P. R.; Guerrero, S. A. *J. Electron Spectrosc. Relat. Phenom.* **1989**, *49*, 281.

(3) Distefano, G.; Granozzi, G.; Olivato, P. R. *J. Chem. Soc., Perkin Trans. 2* **1985**, 2037.

(4) Jones, D.; Modelli, A.; Olivato, P. R.; Dal Colle, M.; de Palo, M.; Distefano, G. *J. Chem. Soc., Perkin Trans. 2* **1994**, 1651.

(5) Distefano, G.; Dal Colle, M.; de Palo, M.; Jones, D.; Bombieri, G.; Del Pra, A.; Olivato, P. R.; Mondino, M. G. *J. Chem. Soc., Perkin Trans. 2* **1996**, 1661.

(6) Dal Colle, M.; Bertolasi, V.; de Palo, M.; Distefano, G.; Jones, D.; Modelli, A.; Olivato, P. R. *J. Phys. Chem.* **1995**, *99*, 15011.

(7) Olivato, P. R.; Mondino, M. G.; Yreijo, M. H.; Wladislaw, B.; Bjorklund, M. B.; Marzorati, L.; Distefano, G.; Dal Colle, M.; Bombieri, G.; Del Pra, A. *J. Chem. Soc., Perkin Trans. 2* **1998**, 109.

(8) Olivato, P. R.; Ribeiro, D. S.; Rittner, R.; Hase, Y.; Del Pra, A.; Bombieri, G. *Spectrochim. Acta, Part A* **1995**, *51*, 1479.

(9) Dargelos, A.; Sandorfy, C. *J. Chem. Phys.* **1977**, *67*, 3011.

(10) Kimura, K.; Katsumata, S.; Achiba, Y.; Yamazaky, T.; Iwata, S. *Handbook of HeI Photoelectron Spectra of Fundamental Organic Molecules*; John Wiley & Sons: New York, 1981.

(11) Wagner, G.; Bock, H. *Chem. Ber.* **1974**, *107*, 6877.

(12) Sance, L.; Schulz, G. J. *J. Phys. Rev. A* **1972**, *5*, 1672.

(13) Modelli, A.; Jones, D.; Distefano, G. *Chem. Phys. Lett.* **1982**, *86*, 434.

(14) Johnston, A. R.; Burrow, P. D. *J. Electron Spectrosc. Relat. Phenom.* **1982**, *25*, 119.

(15) Modelli, A.; Foffani, A.; Scagnolari, F.; Jones, D. *Chem. Phys. Lett.* **1989**, *163*, 269.

(16) Frisch, M. J.; Trucks, G. W.; Schlegel, H. B.; Gill, P. M. W.; Johnson, B. G.; Robb, M. A.; Cheeseman, J. R.; Keith, T.; Petersson, G. A.; Montgomery, J. A.; Raghavachari, K.; Al-Laham, M. A.; Zakrzewski, V. G.; Ortiz, J. V.; Foresman, J. B.; Cioslowski, J.; Stefanov, B. B.; Nanayakkara, A.; Challacombe, M.; Peng, C. Y.; Ayala, P. Y.; Chen, W.; Wong, M. W.; Andres, J. L.; Replogle, E. S.; Gomperts, R.; Martin, R. L.; Fox, D. J.; Binkley, J. S.; Defrees, D. J.; Baker, J.; Stewart, J. P.; Head-Gordon, M.; Gonzales, C.; Pople, J. A. *Gaussian 94*, Revision D4; Gaussian, Inc.: Pittsburgh, PA, 1995.

(17) Bierlein, T. K.; Lingafelter, E. C. *Acta Crystallogr.* **1951**, *4*, 450.

(18) *CRC Handbook of Chemistry and Physics*, 73rd ed.; Lide, D. R., Ed.; CRC Press: Boca Raton, FL, 1992−1993.

(19) Bondi, A. *J. Phys. Chem.* **1964**, *68*, 441.

(20) Modelli, A.; Scagnolari, F.; Distefano, G.; Guerra, M.; Jones, D. *Chem. Phys.* **1990**, *145*, 89.

(21) Modelli, A.; Scagnolari, F.; Distefano, G.; Jones, D.; Guerra, M. *J. Chem. Phys.* **1992**, *96*, 2061.

(22) Modelli, A.; Jones, D.; Colonna, F. P.; Distefano, G. *Chem. Phys.* **1983**, *77*, 153.

(23) Olivato, P. R.; Guerrero, S. G.; Modelli, A.; Granozzi, G.; Jones, D.; Distefano, G. *J. Chem. Soc., Perkin Trans. 2* **1984**, 1505.

(24) Guerra, M.; Distefano, G.; Jones, D.; Colonna, F. P.; Modelli, A. *Chem. Phys.* **1984**, *91*, 383.

(25) Dannenberg, J. J.; Rios, R. *J. Phys. Chem.* **1994**, *98*, 6714.

(26) Kuleshova, L. N.; Zorkii, P. M. *Acta Crystallogr.* **1981**, *B37*, 1363.

(27) The present IE values slightly differ from those (9.67 and 10.46 eV, respectively) previously reported in ref 9.

(28) Koopmans, T. *Physica* **1933**, *1*, 104.

(29) Distefano, G.; de Palo, M.; Dal Colle, M.; Modelli, A.; Jones, D.; Favaretto, L. *J. Mol. Struct. THEOCHEM* **1997**, *418*, 99.

(30) Modelli, A.; Jones, D.; Rossini, S.; Distefano, G. *Tetrahedron* **1984**, *40*, 3257.

(31) Modelli, A.; Distefano, G.; Guerra, M.; Jones, D.; Rossini, S. *Chem. Phys. Lett.* **1986**, *132*, 448.

(32) Modelli, A.; Distefano, G.; Jones, D.; Seconi, G. *J. Electron Spectrosc. Relat. Phenom.* **1983**, *31*, 63.

(33) Guerra, M. *Chem. Phys. Lett.* **1990**, *167*, 315.